Acta Cryst. (1996). B52, 939–953

An Extension of the Voronoi Analysis of Crystal Structures

NOEL W. THOMAS

School of Materials, University of Leeds, Leeds LS2 9JT, England. E-mail: n.w.thomas@leeds.ac.uk

(Received 12 March 1996; accepted 8 July 1996)

Abstract

The Voronoi method of constructing polyhedra about all atoms in a given crystal structure is extended to provide a general, quantitative and concise means of discriminating crystal structures from one another. Although applicable to all crystal structural types, the methodology is developed here by reference to binary non-molecular inorganic systems, A_mB_n, corresponding mainly to ionic crystals and intermetallic compounds. Consideration is given to the geometrical forms of the Voronoi polyhedra, with AB_2 compounds singled out for illustrative purposes. Two methods are proposed for summarizing structural geometry: (i) the use of representative points for elements of Voronoi polyhedra (*i.e.* corners, edges and faces) and relating these to space-group symmetry; (ii) calculation of the ratio of the volumes of Voronoi polyhedra, V_A^V/V_B^V. Topological structural properties (*i.e.* numbers of $A\cdots A$, $A\cdots B$ and $B\cdots B$ pairwise interactions), by comparison, may be quantified by the indices I_{AA}, I_{AB}, I_{BA} and I_{BB}, whose meanings are defined and elucidated. By adopting statistically disordered structures as reference points, indices I'_{AA}, I'_{AB}, I'_{BA} and I'_{BB} are defined, which lead to the generation of two-dimensional topological structure diagrams with I'_{AA} and I'_{BB} as axes. Alternatively, geometrical–topological diagrams may be generated, with V_A^V/V_B^V and $I'_{AA} - I'_{BB}$ as axes. The straightforward modifications required for a chemical–geometrical rather than a topological–geometrical analysis are also described. It is anticipated that the technique will find widespread application in solid-state chemistry and materials science.

1. Introduction

1.1. *Historical perspective*

Polyhedra, and their relevance to our understanding of the natural world, have been a matter of fascination and speculation for over 2000 years. It was Plato who first supposed that the basic elements of earth, air, fire and water had the forms of regular polyhedra, whose constituent triangles were regrouped in transitions between the four elements.* Kepler, in the early seventeenth century, proposed that crystals could be regarded as aggregations of space-filling polyhedra, which, in turn, could be obtained by uniformly compressing arrays of spheres (Kepler, 1611). Later work by Haüy in the nineteenth century developed the view that crystals were arrays of elementary blocks, which could be grouped into shapes that filled space (Haüy, 1822). The nature of possible space-filling polyhedra was subsequently addressed in 1885 by Fedorov, who identified the cube, hexagonal prism, rhombic dodecahedron, elongated dodecahedron and truncated octahedron as the five polyhedra which could fill space when positioned face-to-face in parallel arrays (Senechal, 1990).

Quite independently of these speculations concerning crystals, the mathematician Dirichlet (1850) had developed a geometrical construction to assist in the reduction of quadratic forms, a theme which was later taken up by Voronoi (1908). The construction of Dirichlet domains/Voronoi polyhedra in crystallography was independently taken up by Niggli (1927, 1928), who considered two-dimensional juxtapositions of symmetry elements and circles, and described the *Wirkungsbereich* of a given point as that region of space uniquely belonging to it. He further defined a method whereby convex (Voronoi) polyhedra could be constructed, one for each point. This was based on the construction of planes bisecting at right angles the straight lines joining the point of interest with neighbouring equivalent points. This construction can also be used to divide a lattice into primitive cells centred about the lattice points, as an alternative to the conventional parallelipipedal unit cells. These cells are given various names, *i.e.* Dirichlet regions, Voronoi polyhedra, *Wirkungsbereiche*, Wigner–Seitz cells, or in reciprocal space, first Brillouin zones.

Frank & Kasper (1958) were the first to apply the concept of the Voronoi polyhedron to point atoms, which were symmetrically inequivalent in a crystal structure. By exploiting the correspondence between faces of atomic Voronoi polyhedra and interactions with coordinating atoms, they argued that the Voronoi polyhedron of an atom could be used to determine its coordination number unambiguously. Hoppe (1970) developed this approach by extending the Voronoi construction for points to spheres of finite and unequal radii, these corresponding more closely to atoms or ions. He proposed that the planes of such Voronoi polyhedra should still be perpendicular to the lines joining the centres of the spheres, but that these lines be divided by the planes

* Plato (427–347 BC), Timaeus dialogue, Sections 19–22.

in proportion to the two relevant spherical radii, r_A and r_B. The disadvantages of this construction were subsequently pointed out by Fischer, Koch & Hellner (1971), who demonstrated, in a two-dimensional projection, that regions of space could appear which were not uniquely assigned to a particular *Wirkungsbereich* (Fig. 1*a*). Thus, the requirement of space-filling could not necessarily be fulfilled. Consequently, another method of constructing *Wirkungsbereiche* was proposed by them, based on *Potenzebenen* ('radical planes'). In this connection, any point lying on a such a plane is equidistant from both defining spheres along tangents to those spheres (Fig. 1*b*). Significantly, this construction permits the division of space without areas *XYZ*, as in Fig. 1(*a*). Although any radical plane does lie closer to the centre of the smaller sphere than to that of the larger sphere, this construction lacks the intuitive directness of Hoppe's method (Fig. 1*a*).

The Voronoi theme was taken up again by Carter (1978), who sought to refine the approach of Frank and Kasper in defining coordination numbers. Despite the rigour of the Frank–Kasper definition of coordination number, it overlooked the inequivalence of the different faces of a given Voronoi polyhedron. Carter proposed a means of dealing with this inequivalence, which resulted in the calculation of non-integral, effective coordination numbers. His methodology was formulated in general terms, whereby

$$1/\mathrm{CN} = (\sum_{1}^{N} s_i^2)/(\sum_{1}^{N} s_i)^2. \qquad (1)$$

Here CN is the calculated coordination number of a given atom, s_i a measure of bond formation with its ith neighbour and N the number of neighbours, *i.e.* faces of its polyhedral atomic volume (PAV) cell. PAV cells differed both from conventional Voronoi polyhedra and from the constructions of Hoppe and Fischer, and Koch and Hellner, in that planes perpendicular to lines linking atom centres were placed midway between spherical atomic surfaces (Fig. 1*c*). Two measures of face valences s_i were considered, first the area of the ith face of the PAV and secondly the volume of the pyramid formed by the ith polyhedral face with the central atom itself as the apex. Mention was also made of a third possible basis for s_i values, based on earlier work by Mackay (1972) on straightforward Voronoi polyhedra (*i.e.* faces bisecting lines between atomic *centres*, Fig. 1*d*), rather than PAV cells. Here, the method rested on a calculation of the solid angles subtended at an atom by all faces of its Voronoi polyhedron.

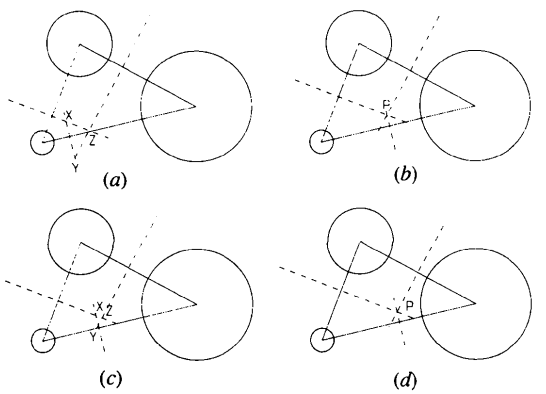

Fig. 1. Two-dimensional analogies for the construction of Voronoi polyhedra: (*a*) taking atomic radii into account by Hoppe's method; (*b*) taking atomic radii into account by the method of Fischer and Koch; (*c*) taking atomic radii into account by Carter's method (PAV cells); (*d*) disregarding atomic radii (unmodified Voronoi construction).

Although the PAV approach offers a more direct method of partitioning space for atoms of unequal radii than the approaches of Fischer or Hoppe, it suffers from the same potential drawback as Hoppe's construction, in that regions of space such as *XYZ* (Fig. 1*c*) can arise, which are not associated with any particular vertex.*

Later work by Fischer & Koch (1979) was concerned with an investigation of packing in organic molecular crystals by the use of Dirichlet domains. With the assumption of idealized covalent radii for atoms, Dirichlet domains enclosed by radical planes were constructed. These workers proceeded to calculate domain volumes and coordination numbers (*i.e.* numbers of faces of domains), disregarding those faces of area less than 2% of the total facial area. *Molecular packing polyhedra* were subsequently constructed, defined as the juxtaposition of atomic Dirichlet domains, with shared faces indicating coordination of one molecule by another. Thus, molecular coordination numbers could be calculated by a method which did not depend explicitly on interaction distances between atoms. Transferable volume increments for atoms in organic molecules were also tabulated (Koch & Fischer, 1980).

More recently, the potential importance of Voronoi polyhedra in intermetallic compounds has been indicated by Nesper (1991), who discussed the possibility that electrons in semi-conducting or intermetallic compounds are concentrated at the face centres or vertices of these polyhedra. He stated further that the detection of voids (*i.e.* vertices of Voronoi polyhedra) and an analysis of their structural meaning would be a significant contribution to the development of a 'comprehensive general structural chemistry'.

1.2. *Scope of the current article*

This article is concerned with extending the Voronoi analysis, both geometrically and topologically. In so

* A comparison of Figs. 1(*a*) and (*c*) shows that the extent of the problem with indeterminate regions *XYZ* is less for PAV cells than for Hoppe's method. This suggests that, provided a suitable means of dealing with such regions has been defined, the PAV is likely to be of widespread applicability. Although well defined mathematically, the radical plane approach (Fig. 1*b*) gives rise to polyhedral boundaries with positions too weakly dependent on the radii of the atoms.

doing, it has two aims: (i) to permit a quantitative comparison of different crystal structural types; (ii) to articulate the influence of stoichiometric and geometrical factors on crystal structure. The methodology is introduced in a stepwise manner, proceeding first from the concept of *complementary Voronoi polyhedra.* Although these polyhedra contain a wealth of structural information, a means is required of conveying its significance concisely. Two strategies are proposed for doing this, the first based on geometry alone, whereby the elements of the Voronoi polyhedra of a structure (*i.e.* vertices, edges and faces) are correlated with its space-group symmetry. The second strategy is to develop a topological framework, which is based on a consideration of whether faces shared between adjacent Voronoi polyhedra are associated with homo- or heteroatomic pairwise interactions.

These topological factors are expressed in terms of *face-interaction indices*, which are calculated, by way of an example, for known structural types of stoichiometry AB_2 amongst ionic crystals and intermetallic compounds. Four face-interaction indices can be calculated for each structure, with two independent indices, permitting the construction of two-dimensional *structure diagrams* for the direct comparison of different structural types. These topological indices can also be combined with geometrical information concerning the sizes of atoms A and B, expressed in terms of the *ratio of the volumes of Voronoi polyhedra*, V_A^V/V_B^V.

The anticipated developments in the Voronoi-based methodology are subsequently discussed, in particular with regard to how the topological framework may be made more sensitive to the *chemistry* of the interactions between neighbouring atoms.

All attributes of the Voronoi polyhedra have been calculated by means of a computer program developed specifically for this purpose, as described in Appendix *B*.

2. The concept of complementary Voronoi polyhedra

The simplest chemical systems correspond to elements for which the structures are best distinguished by comparing their Voronoi polyhedra, as in Table 1. Here the structures are classified in terms of representative elements (sometimes not in their common polymorphs) and the appropriate Pearson symbols. Polyhedral characteristics are described by the numbers of corners C, faces F and edges E, denoted by $C|F|E$. The distribution of the numbers of vertices in the F faces is also given. For example, the notation 24|14|36 6[6] 4[5] 4[4] denotes a polyhedron with 24 vertices, 14 faces and 36 edges. Six faces are hexagonal, four pentagonal and four quadrilateral.

The first 12 structures [Po($cP1$) to Sn($tI4$)] are characterized by only one type of Voronoi polyhedron, which fills space by itself. These 12 polyhedra are shown in Fig. 2, with each polyhedron identified by the column headed 'Fig.' in Table 1. Three common polyhedral types are found: the cube, the rhombic dodecahedron and the truncated octahedron (Figs. 2*a*, *d* and *h*, respectively). The other nine structures in this table are composed of two or more different types of Voronoi polyhedron. In view of their space-filling properties, the polyhedra in a particular structure could be described as *comple-*

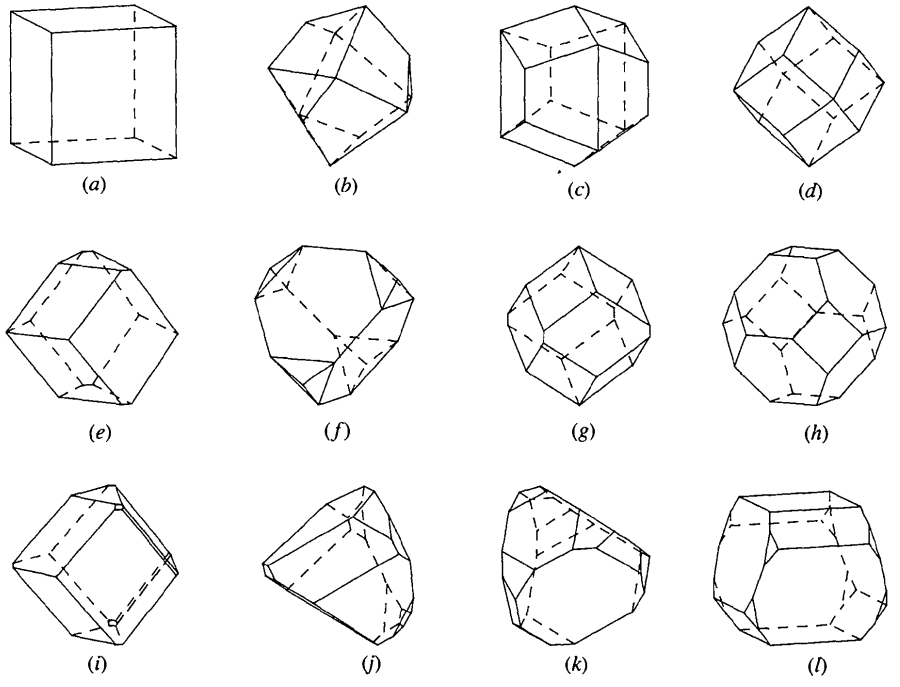

Fig. 2. Self-complementary Voronoi polyhedra of the elemental crystal structures in Table 1.

Table 1. *Voronoi polyhedra in elemental crystal structures*

C|F|E	Faces	Element	Pearson symbol	MDF code	Fig.	Reference
8|6|12	6[4]	Po	cP1	45210	2(*a*)	(1)
12|12|22	8[4] 4[3]	Ga	cI12	51531	2(*b*)	(2)
14|12|24	12[4]	Mg	hP2	38613	2(*c*)	(3)
14|12|24	12[4]	Cu	cF4	22855	2(*d*)	(4)
15|10|23	2[6] 2[5] 6[4]	Ga	oC4	50503	2(*e*)	(5)
16|16|30	4[6] 12[3]	C	cF8	51586	2(*f*)	(6)
18|12|28	4[6] 8[4]	In	tI2	35708	2(*g*)	(7)
24|14|36	8[6] 6[4]	W	cI2	49520	2(*h*)	(8)
24|14|36	6[6] 4[5] 4[4]	Ga	mC4	30010	2(*i*)	(9)
28|16|42	1[10] 7[6] 8[4]	Ga	oC8	30018	2(*j*)	(10)
30|17|45	3[10] 2[6] 12[4]	Si	cI16	51534	2(*k*)	(11)
32|18|48	4[10] 4[6] 2[4] 8[3]	Sn	tI4	48800	2(*l*)	(12)
18|11|27	3[8] 2[6] 6[3]	C	hH4	12896		(13)
20|15|33	3[8] 6[4] 6[3]					
16|10|24	2[6] 4[5] 4[4]	Ga	hR22	51424		(14)
22|13|33	2[7] 2[6] 4[5] 5[4]					
24|15|37	2[7] 8[5] 5[4]					
25|15|38	1[7] 3[6] 7[5] 4[4]					
20|12|30	12[5]	Pu	mC34	49965		(15)
22|13|33	4[6] 6[5] 3[4]					
24|14|36	4[6] 8[5] 2[4]					
26|15|39	6[6] 6[5] 3[4]					
26|15|39	4[6] 10[5] 1[4]					
20|12|30	12[5]	Mn	cP20	38902		(16)
22|14|34	12[5] 2[4]					
20|12|30	5[6] 2[5] 5[4]	Pu	mP16	49726		(17)
24|14|36	8[6] 6[4]					
24|14|36	6[6] 4[5] 4[4]					
28|16|42	9[6] 2[5] 5[4]					
20|12|30	5[6] 2[5] 5[4]	Np	oP8	50082		(18)
28|16|42	7[6] 6[5] 3[4]					
20|12|30	12[5]	Mn	cI58	51558		(19)
24|14|36	3[6] 10[5] 1[4]					
28|16|42	4[6] 12[5]					
20|12|30	1[7] 3[6] 3[5] 5[4]	Ga	oC40	50524		(20)
20|12|30	1[8] 1[7] 2[6] 3[5] 3[4] 2[3]					
26|15|39	1[8] 4[7] 4[5] 4[4] 2[3]					
27|16|41	1[8] 7[6] 2[5] 4[4] 2[3]					
28|16|42	2[10] 2[8] 2[6] 6[4] 4[3]	Ge	tP12	52322		(21)
32|18|48	3[10] 1[8] 2[6] 1[5] 6[4] 3[3]					

References (in CODEN form): (1) JINCAO 28 1837 1966; (2) JCPSA6 68 1221 1978; (3) AMETAR 7 769 1959; (4) JMTSAS 23 757 1988; (5) BUFCAE 84 260 1961; (6) JACGAR 8 457 1975; (7) PSSBBD 107B 245 1981; (8) JAPIAU 42 3288 1971; (9) ACBCAR B25 995 1969; (10) ZKKKAJ 117 293 1962; (11) ACCRA9 17 752 1964; (12) PSSBBD 107B 245 1981; (13) JCFTBS 72 446 1976; (14) ACBCAR 29B 367 1973; (15) ACCRA9 16 369 1963; (16) ACBCAR 34B 3573 1978; (17) ACCRA 9 16 777 1963; (18) ACCRA9 5 660 1952; (19) PRLAAZ 115A 456 1927; (20) ACBCAR 28B 1974 1972; (21) SCIEAS 139 340 1963.

mentary. For example, in the Mn(*cP*20) structure, the 20|12|30 and 22|14|34 polyhedra are complementary.

This concept of *complementary Voronoi polyhedra* is also applicable to non-molecular compounds, since, in the majority of structures, each ion type has a distinct polyhedral type of its own. In order to establish whether the approach of complementary polyhedra could provide a concise framework for comparing alternative structures, 288 different structural types have been examined. These types were taken from the compilation of Pettifor (1986), with crystallographic data for each structural type taken either from the Metals Data File (MDF) or the Inorganic Crystal Structure Database (ICSD). Since each structural type is named after a particular parent composition, *e.g.* $MgCu_2$-type, CaF_2-type, the data analysed corresponded to those of the parent composition itself. The analysis encompassed the following families of binary compounds: 49 AB; 4 A_3B_7; 10 AB_5; 23 A_2B_3; 10 A_2B_5; 8 AB_6; 18 A_3B_4; 42 AB_3; 3 A_2B_{17}; 7A_3B_5; 2 A_6B_{23}; 2 AB_{11}; 85 AB_2; 20 AB_4; 3AB_{12}; 2 AB_{13}.

In summary, 321 different Voronoi polyhedra were identified, this making a concise overview difficult. The polyhedron with the highest number of vertices, 42, was found for zinc ions in the ZnP_2 structure (42|23|63 1[12] 2[11] 1[9] 2[8] 2[6] 2[5] 6[4] 7[3]). The polyhedron with the least number of vertices corresponded to the octahedron (6|8|12 8[3]), which was found in the CaF_2, ThH_2 and Hg_4Pt structure types. Whereas the polyhedra which are complementary to the octahedra are identical in the CaF_2 and ThH_2 structures (16|10|24 6[6] 4[3]),

the Hg_4Pt structure has complementary 12|8|18 6[5] 2[3] polyhedra. This is a direct consequence of the AB_4, rather than AB_2 stoichiometry. The most frequently occurring Voronoi polyhedron is the truncated octahedron (24|14|36 8[6] 6[4]), which arises in 37 out of the 288 structures, with varying degrees of distortion. In the following 19 structures this polyhedron is self-complementary: CsCl, NiO, HgMn, AuCu, AuCd, NaTl, SeTl, CuTi, Ti_3Cu_4, Al_3Os_2, Ti_2Pd_3,Ti_3Pd_5, CaC_2, Cd_2Ce, Au_2V, $MoSi_2$, $CuTi_3$, BiF_3 and $MoNi_4$. In the remaining 18 structures it is found with a range of complementary Voronoi polyhedra.*

Although the identification of *complementary Voronoi polyhedra* is a logical way to proceed, the sheer number of different polyhedral types makes this method too cumbersome for a direct and meaningful comparison of different crystal structures. This is not surprising, since the geometrical forms of the Voronoi polyhedra within just one unit cell, together with the requirement of space-filling, determine the complete crystal structure uniquely. A means is required for systematizing this information, either by relating polyhedral elements to space-group symmetry or by developing a topological classification of structures from their Voronoi polyhedra. These two approaches are now considered in turn.

3. Relating Voronoi polyhedral elements to space-group symmetry

Of the three types of Voronoi polyhedral elements, corners, edges and faces, it is clear that the coordinates of the corners of Voronoi polyhedra $[x_V, y_V, z_V]$, as points in space, are governed by the symmetry of the space group. $[x_V, y_V, z_V]$ values for the $MgCu_2$ structure are quoted in Table 6 in Appendix *C*, with the 136 vertices in the unit cell occupying special positions (96*g*), (32*e*) and (8*b*). By representing Voronoi edges and faces also as points, their numbers and coordinates can also be shown to be governed by space-group symmetry.

If a Voronoi edge links two vertices of inequivalent point symmetry, all intermediate points along that edge will have the same point symmetry as one another. This is because the presence of inequivalent points at both ends of the edge precludes the existence at the edge midpoint of a centre of symmetry, or alternatively a mirror plane or rotation axis perpendicular to the edge direction. If, however, the two vertices have equivalent point symmetry, the point symmetry of the edge midpoint may differ from the point symmetry at all other intermediate points along the edge. Thus, if a unique representative point for a Voronoi edge is required, its midpoint must be taken. Only a point with the symmetry of the midpoint will, in all cases, be generated with the same frequency in the unit cell as the edge-type it represents.

Similar considerations apply to Voronoi faces, the perpendiculars of which join two atoms. If these two atoms have different types, any point on the face-perpendicular will be generated with the same frequency as the perpendicular itself. If, however, the two atoms are identical, only the midpoint of the face-perpendicular is the representative point for the face. These requirements are satisfied, in general, by adopting as the representative point of a Voronoi face that point on the line joining the two atoms which is equidistant from the *surfaces* of both atom spheres. This definition, expressed in terms of distances from atomic surfaces, permits a generalization to PAV cells and not merely conventional Voronoi polyhedra. Wherever the two atoms are identical, the representative point is coincident with the midpoint of the line connecting atomic *centres*.

A justification of the above arguments is to be found in Appendix *A*.

4. A topological classification of crystal structures

4.1. *Definition of face-interaction indices*

If a discrimination between alternative structural types is sought on chemical grounds, an appropriate method rests on a consideration of how the valences (or bonding electrons) of the atoms are distributed over nearest-neighbour interactions. In simple cases, it may be argued that such nearest-neighbour interactions represent chemical bonds. However, more generally, some kind of weighting scheme is required to differentiate between different nearest-neighbour interaction strengths.

The choice of atomic valences is not straightforward, since a knowledge is required of numbers and orbital assignations of the electrons which participate in bonding interactions. A generalized chemical approach to analysing crystal structures would require an analysis of these atomic interactions, which, in binary compounds, A_mB_n, correspond to $A\cdots A$, $A\cdots B$ and $B\cdots B$ interactions. According to such an approach, the atoms may be envisaged as acting as valence sources, with their valence distributed over their interactions (or, more loosely, bonds). In terms of Voronoi polyhedra, the problem is to identify how the forms of the polyhedra determine the distribution of electronic charge over polyhedral faces, which correspond to pairwise interactions. To tackle this problem, use may be made of geometrical attributes such as facial areas, polyhedral volume increments due to faces, solid angles subtended by faces at the atoms at the centres of the polyhedra or distances between atoms and their respective polyhedral faces. Alternatively, a valence-interaction length relationship could be used, arising from the use of appropriate bond-valence parameters (Brown & Altermatt, 1985; Brese & O'Keeffe, 1991; O'Keeffe & Brese, 1992).

* The results of the analysis have been deposited with the IUCr (Reference: AB0351). Copies may be obtained through The Managing Editor, International Union of Crystallography, 5 Abbey Square, Chester CH1 2HU, England.

For each of these possible methods, valence fractions i_{AA} and i_{AB} can be derived for A-atom polyhedra, to represent the proportions of A-atom valence associated with A–A and A–B interactions, respectively. Likewise, valence fractions i_{BA} and i_{BB} will represent, for B-atom polyhedra, the proportions of B-atom valence associated with B–A and B–B interactions, respectively. Thus, $i_{AA} + i_{AB} = 1$ and $i_{BA} + i_{BB} = 1$.

Still proceeding generally, indices I_{AA}, I_{AB}, I_{BA} and I_{BB} may be defined by summing the corresponding i indices over all polyhedra in the unit cell. Thus,

$$I_{AA} = Zmi_{AA};\ I_{AB} = Zmi_{AB}. \tag{2}$$

Similarly

$$I_{BA} = Zni_{BA};\ I_{BB} = Zni_{BB}. \tag{3}$$

It follows that

$$I_{AA} + I_{AB} = Zm;\ I_{BA} + I_{BB} = Zn. \tag{4}$$

I_{AA}, I_{AB}, I_{BA} and I_{BB} are termed face-interaction indices.

4.2. *Method of calculation of face-interaction indices*

In accordance with (2) and (3), the calculation of face-interaction indices I_{AA}, I_{AB}, I_{BA} and I_{BB} requires a knowledge of polyhedral valence fractions i_{AA}, i_{AB}, i_{BA} and i_{BB}, respectively. Values of these will depend on the method used to evaluate the valence fractions of polyhedral faces, as discussed in (i) above. Merely in order to introduce the methodology, the *simplest* approach is adopted here. According to this, all faces of a given Voronoi polyhedron are assigned equal valence fractions, regardless of their different characteristics. Adopting the notation that s_{AA} represents the valence fraction of an A-polyhedral face which is shared with another A polyhedron and s_{AB} the valence fraction of an A-polyhedral face shared with a B polyhedron, this simple approach states that $s_{AA} = s_{AB} = 1/F_A$. Likewise for the valence fractions of B polyhedra, $s_{BA} = s_{BB} = 1/F_B$, where F_A and F_B represent the numbers of faces in polyhedra A and B, respectively.

It is to be noted that face-interaction indices, as defined by this simple method, are directly related to the number of interactions in the unit cell. With respect to A–A interactions,

$$I_{AA} = Zmi_{AA} = N^i_{AA}(2/F_A). \tag{5}$$

Thus, I_{AA} may be derived either by multiplying i_{AA} by the number of A ions in the unit cell or through multiplying the number of A–A interactions in the unit cell, N^i_{AA}, by the net valence fraction per A–A interaction, $2/F_A$. Each A–A interaction valence fraction is made up of a contribution of $1/F_A$ from both polyhedra which share a face perpendicular to that interaction. Similarly,

$$I_{BB} = Zmi_{BB} = N^i_{BB}(2/F_B) \tag{6}$$

and, with respect to heteroatomic interactions,

$$I_{AB} = Zmi_{AB} = N^i_{AB}(1/F_A);\ I_{BA} = Zni_{BA} = N^i_{BA}(1/F_B). \tag{7}$$

Example calculations of i, I and N^i values are to be found in Appendix $C2$, where the simple method of distributing valence fractions equally over faces is followed. It is intended to give a treatment of the calculation of i and I indices by more refined methods in later articles. These will take the geometrical attributes of Voronoi polyhedra into account, either directly [as described in (i) above and in Appendix B] or indirectly, by means of a bond-valence type of approach.

4.3. *Definition and calculation of intrinsic face-interaction indices*

Regardless of the method of calculation of I indices, it is desirable to be able to compensate for the effects of stoichiometry on their values. For example, in any AB_2 structure it is expected that $I_{BB} > I_{AA}$, since there are twice as many B atoms as A atoms. A method is now proposed for deriving intrinsic face-interaction indices, in which the weighting influence of stoichiometry has been removed.

For any given crystal structure a reference structure can be adopted, whereby each atomic position is occupied not by a single atom (as in the crystal structure itself), but by a statistical combination of all atom types in the structure in their stoichiometric proportions. With reference to a binary compound A_mB_n, each statistical atom of this kind, denoted X for the present, will have $i_{XA} = m/(m+n)$ and $i_{XB} = n/(m+n)$, with the second suffix referring either to an A or a B atom. i_{XA} and i_{XB} may be further divided into contributions from A and B atoms, $i_{XA} = i^{\text{ref}}_{AA} + i^{\text{ref}}_{BA}$, where the suffix 'ref' has been added to avoid confusion between i values for actual and reference crystal structures. Here, $i^{\text{ref}}_{AA} = mi_{XA}/(m+n)$ and $i^{\text{ref}}_{BA} = ni_{XA}/(m+n)$. Similarly, $i_{XB} = i^{\text{ref}}_{AB} + i^{\text{ref}}_{BB}$, whereby $i^{\text{ref}}_{AB} = mi_{XB}/(m+n)$ and $i^{\text{ref}}_{BB} = ni_{XB}/(m+n)$.

It follows that, for each statistical atom in the unit cell, the following i values are obtained

$$\begin{aligned} &i^{\text{ref}}_{AA} = m^2/(m+n)^2;\ i^{\text{ref}}_{AB} = mn/(m+n)^2 \\ &i^{\text{ref}}_{BA} = mn/(m+n)^2;\ i^{\text{ref}}_{BB} = n^2/(m+n)^2. \end{aligned} \tag{8}$$

I indices for the reference structure are obtained by summing i indices over all $Z(m+n)$ atomic positions. Thus,

$$\begin{aligned} &I^{\text{ref}}_{AA} = Zm^2/(m+n);\ I^{\text{ref}}_{AB} = Zmn/(m+n) \\ &I^{\text{ref}}_{BA} = Zmn/(m+n);\ I^{\text{ref}}_{BB} = Zn^2/(m+n). \end{aligned} \tag{9}$$

Note that these I indices for the reference structure also satisfy (4) and that $I^{\text{ref}}_{AB} = I^{\text{ref}}_{BA}$. Intrinsic face-interaction

Table 2. *Values of raw and intrinsic face-interaction indices and Voronoi polyhedral volume ratios for the 85 AB_2 structural types*

Columns headed Fig. 3(*a*) and Fig. 4 identify, where necessary, points in these figures.

System	I_{AA}	I_{AB}	I_{BA}	I_{BB}	I'_{AA}	I'_{AB}	I'_{BA}	I'_{BB}	$V_A^V V_B^V$	MDF code	Ref.	Fig. 3(*a*)	Fig. 4
$CaIn_2$	0.2857	1.7143	2.1818	1.8182	0.4286	1.2857	1.6364	0.6818	1.1180	51010	1		P
$CeCu_2$	1.3333	2.6667	4.3636	3.6364	1.0000	1.0000	1.6364	0.6818	1.2066	16494	2		qq
AlB_2	0.4000	0.6000	1.0909	0.9091	1.2000	0.9000	1.6364	0.6818	1.3649	1461	3	a	uu
$ThSi_2$	1.6000	2.4000	4.3636	3.6364	1.2000	0.9000	1.6364	0.6818	1.2384	50866	4	a	tt
$MgCu_2$	2.0000	6.0000	8.0000	8.0000	0.7500	1.1250	1.5000	0.7500	1.2298	24078	5	b	ff
$MgNi_2$	2.0000	6.0000	8.0000	8.0000	0.7500	1.1250	1.5000	0.7500	1.2279	38650	6	b	ff
$MgZn_2$	1.0000	3.0000	4.0000	4.0000	0.7500	1.1250	1.5000	0.7500	1.2253	38892	7	b	ff
Cu_2Sb	0.8889	1.1111	1.8667	2.1333	1.3334	0.8333	1.4000	0.8000	1.1956	24758	8		ss
ZnP_2	2.0870	5.9130	7.3450	8.6550	0.7826	1.1087	1.3772	0.8114	1.1240	50763	9		cc
Ni_2In	0.0000	2.0000	1.7662	2.2338	0.0000	1.5000	1.3247	0.8377	0.9805	36005	10		z
CuP_2	0.8421	3.1579	3.4379	4.5621	0.6316	1.1842	1.2892	0.8554	1.0822	24393	11		O
Cd_2Ce	0.1429	0.8571	0.8571	1.1429	0.4287	1.2856	1.2856	0.8572	1.0403	50991	12		I
Co_2Si	1.0667	2.9333	3.2527	4.7473	0.0800	1.1000	1.2198	0.8901	1.0406	50110	13		Z
CaF_2	0.0000	4.0000	3.2000	4.8000	0.0000	1.5000	1.2000	0.9000	0.7826	24926*	14	c	v
ThH_2	0.0000	2.0000	1.6000	2.4000	0.0000	1.5000	1.2000	0.9000	0.8119	34370	15	c	w
$PtHg_2$	0.2000	0.8000	0.8000	1.2000	0.6000	1.2000	1.2000	0.9000	0.7116	35043	16	d	J
Ag_2O	0.4000	1.6000	1.6000	2.4000	0.6000	1.2000	1.2000	0.9000	0.7090	1020	17	d	J
$FeSi_2$	0.3333	0.6667	0.8000	1.2000	0.9999	1.0001	1.2000	0.9000	0.7726	29340	18		hh
RuB_2	0.8571	1.1429	1.6000	2.4000	1.2856	0.8572	1.2000	0.9000	1.2028	10882	19		rr
Pt_2Ga	2.4048	5.5952	6.3516	9.6484	0.9018	1.0491	1.1909	0.9045	0.9841	50205	20		dd
$ZrGa_2$	1.3333	2.6667	2.9524	5.0476	1.0000	1.0000	1.1072	0.9464	1.0160	50431	21		jj
$BaSi_2$	3.1455	4.8545	5.8413	10.1587	1.1796	0.9102	1.0952	0.9524	1.2864	50211	22		oo
$SmSb_2$	2.5000	5.5000	5.7778	10.2222	0.9375	1.0313	1.0833	0.9583	0.9865	50480	23		aa
$MoPt_2$	0.3333	1.6667	1.4286	2.5714	0.5000	1.2500	1.0715	0.9643	0.9669	40157	24		G
CaC_2	0.5714	1.4286	1.4286	2.5714	0.8571	1.0715	1.0715	0.9643	1.1457	12904	25	e	Y
Au_2V	1.1429	2.8571	2.8571	5.1429	0.8572	1.0714	1.0714	0.9643	1.0111	50428	26	e	X
$TiSi_2$	2.2857	5.7143	5.7143	10.2857	0.8571	1.0714	1.0714	0.9643	1.0062	48491	27	e	W
$MoSi_2$	0.5714	1.4286	1.4286	2.5714	0.8571	1.0715	1.0715	0.9643	1.0010	40418	28	e	W
$CrSi_2$	0.8571	2.1429	2.1429	3.8571	0.8571	1.0715	1.0715	0.9643	0.9996	22495	29	e	W
$CaSi_2$	2.2500	3.7500	4.2462	7.7538	1.1250	0.9375	1.0615	0.9692	1.2839	15227	30		nn
Ag_2Te	1.0667	2.9333	2.8070	5.1930	0.8000	1.1000	1.0526	0.9737	1.0334	1305	31		Q
FeS_2 (pyrite)	0.0000	4.0000	2.8000	5.2000	0.0000	1.5000	1.0500	0.9750	0.8330	29099	32		u
Ti_2Ni	8.0000	24.0000	21.7143	42.2857	0.7500	1.1250	1.0179	0.9911	0.8452	42987	33		N
FeS_2 (marcasite)	0.0000	2.0000	1.3333	2.6667	0.0000	1.5000	1.0000	1.0000	0.7808	50078	34		s
$PdCl_2$	0.3333	1.6667	1.3333	2.6667	0.5000	1.2500	1.0000	1.0000	0.9529	14580*	35	f	F
ThC_2	0.6667	3.3333	2.6667	5.3333	0.5000	1.2500	1.0000	1.0000	1.1038	14507	36	f	H
$HfGa_2$	5.3333	10.6667	10.6667	21.3333	1.0000	1.0000	1.0000	1.0000	1.0200	30117	37		ee
$CaSb_2$	0.5714	1.4286	1.3214	2.6786	0.8571	1.0715	0.9910	1.0045	1.0414	49686	38		T
$SrBr_2$	0.0000	10.0000	6.4762	13.5238	0.0000	1.5000	0.9714	1.0143	0.7958	18487*	39		t
Pd_2As	2.3273	5.6727	5.1691	10.8309	0.8727	1.0636	0.9692	1.0154	0.9310	6676	40		S
BaS_2	0.0000	4.0000	2.5263	5.4737	0.0000	1.5000	0.9474	1.0263	1.0258	11616	41	g	r
$PdSe_2$	0.0000	4.0000	2.5263	5.4737	0.0000	1.5000	0.9474	1.0263	0.8544	44875	42	g	q
SiS_2	0.5714	3.4286	2.5263	5.4737	0.4286	1.2857	0.9474	1.0263	0.5518	46951	43		A
La_2Sb	1.2308	2.7692	2.5098	5.4902	0.9231	1.0385	0.9412	1.0294	0.9145	37833	44		V
CS_2	0.0000	4.0000	2.5000	5.5000	0.0000	1.5000	0.9375	1.0313	0.6643	50434	45	g	p
$ZrSi_2$	1.5000	2.5000	2.5000	5.5000	2.1250	0.9375	0.9375	1.0313	1.0191	48707	46	g	ii
ZrO_2	0.0000	4.0000	2.4762	5.5238	0.0000	1.5000	0.9286	1.0357	0.7284	32612*	47	g	n
SrI_2	0.0000	8.0000	4.9524	11.0476	0.0000	1.5000	0.9286	1.0357	0.7759	17043*	48	g	o
Li_2Sb	1.0909	4.9091	3.7143	8.2857	0.5454	1.2273	0.9286	1.0357	0.9296	51138	49		E
$NdAs_2$	1.3333	2.6667	2.4265	5.5735	1.0000	1.0000	0.9099	1.0450	1.0365	49706	50		bb
As_2Ge	3.3667	4.6333	4.6944	11.3056	1.2625	0.8687	0.8802	1.0599	0.8448	50219	51		kk
Fe_2P	0.7143	2.2857	1.7395	4.2605	0.7143	1.1428	0.8697	1.0651	0.8764	28873	52		M
ReB_2	0.8571	1.1429	1.1429	2.8571	1.2856	0.8572	0.8572	1.0714	1.2545	51023	53	h	mm
$HoSB_2$	0.8571	1.1429	1.1429	2.8571	1.2856	0.8572	0.8572	1.0714	1.0303	50414	54	h	ll
Ta_2P	3.8095	8.1905	6.7025	17.2975	0.9524	1.0238	0.8378	1.0811	0.8693	50283	55		R
$IrSe_2$	0.0000	8.0000	4.4667	11.5333	0.0000	1.5000	0.8375	1.0812	0.7183	36910	56	i	m
TiO_2 (rutile)	0.0000	2.0000	1.1111	2.8889	0.0000	1.5000	0.8333	1.0833	0.6444	28207*	57	i	l
$ZrSb_2$	2.7692	5.2308	4.4118	11.5882	1.0385	0.9808	0.8272	1.0864	0.8712	50196	58		U
$CuMg_2$	3.2000	12.8000	8.5333	23.4667	0.6000	1.2000	0.8000	1.1000	0.7519	24080	59	j	C
Al_2Cu	0.8000	3.2000	2.1333	5.8667	0.6000	1.2000	0.8000	1.1000	0.7827	2301	60	j	D
$FeSb_2$	0.4000	1.6000	1.0667	2.9333	0.6000	1.2000	0.8000	1.1000	0.7653	50073	61	j	C
VO_2	0.4000	3.6000	2.1176	5.8824	0.3000	1.3500	0.7941	1.1030	0.6521	43637	62		y
$OsGe_2$	1.0909	2.9091	2.1071	5.8929	0.8182	1.0909	0.7902	1.1049	0.8655	49872	63	k	L

Table 2 (*cont.*)

System	I_{AA}	I_{AB}	I_{BA}	I_{BB}	I'_{AA}	I'_{AB}	I'_{BA}	I'_{BB}	$V_A^V V_B^V$	MDF code	Ref.	Fig. 3(*a*)	Fig. 4
$NbSb_2$	1.0909	2.9091	2.1071	5.8929	0.8182	1.0909	0.7902	1.1049	0.8413	41363	64	k	K
SiO_2 (coesite)	1.5273	14.4727	8.0511	23.9489	0.2864	1.3568	0.7548	1.1226	0.5184	21622*	65		x
$CuCl_2$	0.0000	2.0000	1.0000	3.0000	0.0000	1.5000	0.7500	1.1250	0.6036	35971*	66	l	i
V_2N	0.0000	3.0000	1.5000	4.5000	0.0000	1.5000	0.7500	1.1250	0.6537	51064	67	l	j
$CdCl_2$	0.0000	1.0000	0.5000	1.5000	0.0000	1.5000	0.7500	1.1250	0.7367	27117*	68	l	k
SiO_2 (l.cristobalite)	0.0000	4.0000	2.0000	6.0000	0.0000	1.5000	0.7500	1.1250	0.3974	17256*	69	l	g
$CoSb_2$	0.8000	3.2000	1.9683	6.0317	0.6000	1.2000	0.7381	1.1309	0.7491	20594	70		B
SiO_2 (l.quartz)	0.0000	3.0000	1.4286	4.5714	0.0000	1.5000	0.7143	1.1428	0.4645	21232*	71	m	h
$CaCl_2$	0.0000	2.0000	0.9412	3.0588	0.0000	1.5000	0.7059	1.1471	0.6604	11396*	72	m	j
Fe_2C	0.0000	2.0000	0.9412	3.0588	0.0000	1.5000	0.7059	1.1471	0.6703	50077	73	m	j
$NbTe_2$	2.4545	3.5455	2.8000	9.2000	1.2272	0.8864	0.7000	1.1500	0.7134	49893	74		gg
MoS_2	1.0000	1.0000	0.9231	3.0769	1.5000	0.7500	0.6923	1.1538	0.6951	40237	75	n	pp
Nbs_2	1.0000	1.0000	0.9231	3.0769	1.5000	0.7500	0.6923	1.1538	0.6819	41323	76	n	pp
TiO_2(II)	0.0000	4.0000	1.7778	6.2222	0.0000	1.5000	0.6667	1.1667	0.6690	29514*	77	o	j
PbO_2	0.0000	4.0000	1.7778	6.2222	0.0000	1.5000	0.6667	1.1667	0.6974	50107	78	o	j
TiO_2 (brookite)	0.0000	8.0000	3.3824	12.6176	0.0000	1.5000	0.6342	1.1829	0.6260	18398*	79		f
SiO_2 (keatite)	0.0000	12.0000	4.8391	19.1609	0.0000	1.5000	0.6049	1.1976	0.4302	17232*	80	p	d
CdI_2	0.0000	1.0000	0.4000	1.6000	0.0000	1.5000	0.6000	1.2000	0.6640	52280	81	p	e
Fe_2N	0.0000	3.0000	1.2000	4.8000	0.0000	1.5000	0.6000	1.2000	0.6672	28495	82	p	e
SiO_2 (l.tridymite)	0.0000	48.0000	18.5694	77.4306	0.0000	1.5000	0.5803	1.2099	0.3807	786*	83	p	a
SiO_2 (h.quartz)	0.0000	3.0000	1.1429	4.8571	0.0000	1.5000	0.5715	1.2143	0.4209	37266*	84	p	b
TiO_2 (anatase)	0.0000	4.0000	1.4118	6.5882	0.0000	1.5000	0.5294	1.2353	0.5760	28208*	85		c

† Code-numbers followed by an asterix refer to the ICSD (Inorganic Crystal Structure Database) and not the MDF (Metals Data File). References (in CODEN form): (1) ZAACAB 330 221 1964; (2) JCOMAH 30 237 1973; (3) JAPUAW 44 970 1971; (4) ZAACAB 249 325 1942; (5) JSSCBI 30 209 1979; (6) ACBCAR 36B 1548 1980; (7) ACHSE7 43 296 1989; (8) AKMGAE 12B 1 1935; (9) JPCSAW 24 333 1963; (10) MSCEAA 22 133 1976; (11) ZAACAB 491 225 1982; (12) GCITA9 84 463 1954; (13) ACCRA9 8 83 1955; (14) JCPSA 41 2324 1964; (15) ACCRA9 15 287 1962; (16) MOCMB7 84 211 1953; (17) JACTAW 55 25 1972; (18) ACSAA4 14 1414 1960; (19) ACSAA4 17 2036 1963; (20) MTLLAF 28 1160 1974; (21) ZEMTAE 53 474 1962; (22) ACIEAY 2 393 1963; (23) INOCAJ 6 1685 1967; (24) ZEMTAE 55 619 1964; (25) JCPSA6 35 1950 1961; (26) ZEMTAE 53 433 1962; (27) ACBCAR B33 2347 1977; (28) SSCOA4 55 629 1985; (29) AKMGAE 11A 10 1933; (30) JSSCBI 28 369 1979; (31) ZEKGAX 112 44 1959; (32) MRSPDH 22 49 1984; (33) TMSAAB 227 674 1963; (34) ZKKKAJ 97A 504 1937; (35) ZEKGA 100 189 1938; (36) ACBCAR 24B 1121 1968; (37) NATWAY 49 57 1962; (38) ZAACAB 425 104 1976; (39) JSSCB 46 313 1983; (40) JCOMAH 19 300 1969; (41) ACBCAR B31 2905 1975; (42) NATWAY 44 229 1957; (43) ACBCAR 38B 1270 1982; (44) ACBCAR 36B 220 1980; (45) JCPSA 48 2974 1968; (46) 00ACAS 57 8 1955; (47) JACTA 73 2828 1990; (48) ZAACA 369 62 1969; (49) ZNBAD2 32B 357 1977; (50) ACBCAR 34B 1959 1978; (51) ACCRA9 15 167 1962; (52) JUPSAU 46 1616 1979; (53) ACCRA9 15 97 1962; (54) INOCAJ 10 2089 1971; (55) ACSAA4 20 2393 1966; (56) JSSCBI 89 315 1990; (57) JACSA 109 3639 1987; (58) ACSAA4 26 1633 1972; (59) NATWAY 38 46 1951; (60) JSSCBI 83 370 1989; (61) ASAA4 23 3043 1969; (62) ACSAA4 24 420 1970; (63) ZEMTAE 51 238 1960; (64) NATUAS 203 512 1964; (65) AMMIA 66 324 1981; (66) AMMIA 78 187 1993; (67) ACBCAR 35B 2677 1979; (68) JSSCB 19 6761 1986; (69) ZEKGA 138 274 1973; (70) ACSAA4 25 411 1971; (71) AMMIA 65 920 1980; (72) TACAA 6 57 1970; (73) AMETAR 20 645 1972; (74) ACCRA9 20 264 1966; (75) CJPHAD 61 76 1983; (76) JSSCBI 37 140 1981; (77) MRBUA 23 743 1988; (78) ZFKHA9 26 743 1952; (79) CAMIA 17 77 1979; (80) ZEKGA 112 409 1959; (81) XNBSAV 44C 233 1969; (82) MITLAC 49 195 1957; (83) ACBCA 33 2615 1977; (84) JALCE 197 137 1993; (85) JACSA 109 3639 1987.

indices I'_{AA}, I'_{AB}, I'_{BA} and I'_{BB} may now be defined as

$$I'_{AA} = I_{AA}/I^{\text{ref}}_{AA};\ I'_{AB} = I_{AB}/I^{\text{ref}}_{AB}$$
$$I'_{BA} = I_{BA}/I^{\text{ref}}_{BA};I'_{BB} = I_{BB}/I^{\text{ref}}_{BB}. \qquad (10)$$

5. Generation of topological and geometrical–topological structure diagrams

On the basis of the intrinsic face-interaction indices defined in (10), it is possible to generate two-dimensional topological structure diagrams, whereby each structural type may be represented as a point. The requirement of a two-dimensional diagram follows from (4), (9) and (10), as it may be shown that the values of I'_{AA} and I'_{AB} are interdependent, as are the values of I'_{BA} and I'_{BB}. The pair of values (I'_{AA} and I'_{BB}) thus determines the numbers and types of interactions in a given structure unambiguously. Substitution of (9) into (10), together with the application of conditions (4), leads to the following results

$$I'_{AB} = 1 + (m/n)(1 - I'_{AA})$$
$$I'_{BA} = 1 + (n/m)(1 - I'_{BB}). \qquad (11)$$

Rather than present a full topological characterization of all 288 binary structural types, attention is focused here on the largest subset, that corresponding to stoichiometry AB_2. Calculated I and I' values are given in Table 2, where it is observed that the sums $I_{AA} + I_{AB}$ and $I_{BA} + I_{BB}$ are always integral, in accordance with (4). Fig. 3(*a*) is a two-dimensional topological structure diagram of the 85 AB_2 structural types, with I'_{AA} and I'_{BB} as axes. In general, the structural types are well separated, with points in all four quadrants of the diagram. Salt-like structures, *i.e.* those made up of cation coordination

polyhedra, have $I'_{AA} = 0$. Thus, they are located on the vertical I'_{BB} axis. Worthy of note is the clustering of points around the $(I'_{AA}, I'_{BB}) = (1,1)$ axial intersection: provided that the relative sizes of A and B atoms are similar, these structural types are predicted to be susceptible to order–disorder transformations, since $I_{AA} \simeq I_{AA}^{ref}$ and $I_{BB} \simeq I_{BB}^{ref}$. $HfGa_2$, in particular, with $I'_{AA} = I'_{BB} = 1$ and $V_A^V/V_B^V = 1.0200$ (*i.e.* similar Voronoi polyhedral volumes of Hf and Ga ions), is likely to be susceptible to such a transformation.

The following broad interpretation may be given for the positions of points in the diagram: structures in the bottom-left quadrant have I'_{AA}, $I'_{BB} < 1$, indicating a tendency for coordination of A atoms by B atoms and B atoms by A atoms, *i.e.* good mixing of dissimilar ion types. Interestingly, the structural types with the lowest (I'_{AA}, I'_{BB}) values, Ni_2In and $CaIn_2$, both contain indium. The top-left quadrant includes structures based on coordination polyhedra at the far left (*i.e.* $I'_{AA} = 0$), whereby interactions between the B atoms forming the coordination polyhedra (generally anions) give rise to large I'_{BB} values. A tendency towards such structures is maintained in the top-left quadrant, this diminishing with increasing values of I'_{AA}. It is to be noted that the effect of stoichiometry is marked, since no structures are observed with $I'_{BB} = 0$, which would correspond to the component in stoichiometric excess being coordinated exclusively by the minority component. Structural types in the bottom-right quadrant are characterized by significant nearest-neighbour interactions between minority A ions, which occur at the expense of $B\cdots B$ interactions. Furthermore, structures in the top-right quadrant display poor mixing of A and B components, with a tendency towards homoatomic $A\cdots A$ and $B\cdots B$ interactions.

Insight into the geometrical basis of some of these observations is provided by Fig. 3(*b*). Here, the plotted

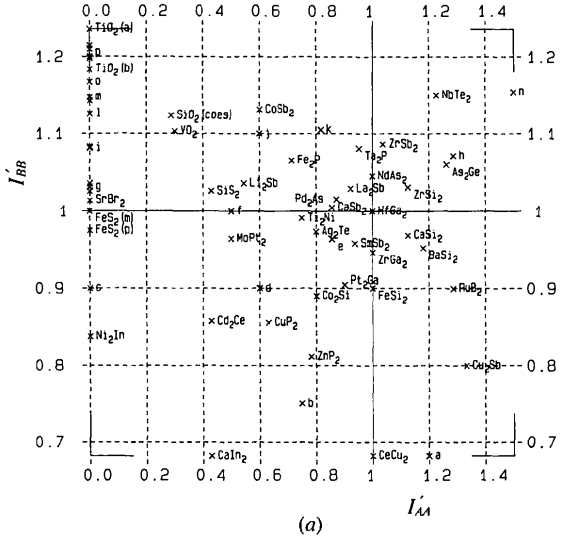

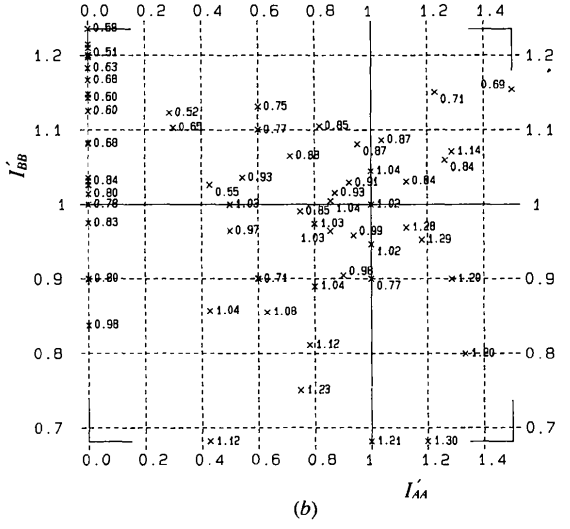

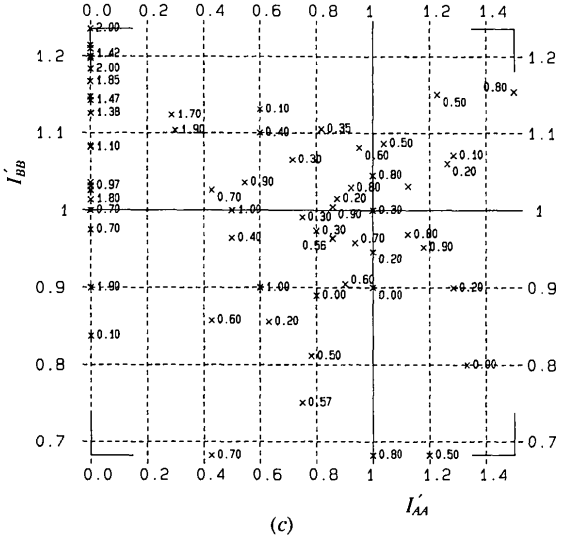

Fig. 3. (*a*) Topological structure diagram for the 85 AB_2 structural types in Table 2. Chemical compositions are indicated wherever space allows. Otherwise points are labelled with characters a–p, which can be correlated with compositions in Table 2. (*b*) Identical structure diagram to (*a*), but with the points labelled by values of Voronoi polyhedral volume ratios, V_A^V/V_B^V. Overlapping or clustered points are labelled with mean values for contributing points. (*c*) Identical structure diagram to (*a*) and (*b*), but with points labelled by values of absolute electronegativity differences (Pauling scale) of the appropriate compositions $|\chi_A - \chi_B|$. Overlapping or clustered points are labelled with mean values for contributing points.

points are identical to those in Fig. 3(*a*), but they are labelled by values of V_A^V/V_B^V, the ratio of the volumes of Voronoi polyhedra. This ratio is chosen to represent the geometry of a given structural type, since its value is dependent on the atomic coordinates of constituent ions and not their radii. Thus, to a good approximation, V_A^V/V_B^V is representative of a structural type, regardless of the particular composition concerned. The approximation being made here is that the atomic coordinates of the parent composition of a structural type, which have been used to calculate the V_A^V/V_B^V values in Table 2, are representative of all compositions of that type. In some structural types, *e.g.* $MgCu_2$, the ions occupy special positions with invariant coordinates, so that V_A^V/V_B^V is constant for all structures of that type. In a structural type where some or all the ions occupy positions with variable coordinates, some variation in V_A^V/V_B^V values will be observed between alternative compositions. For this reason, some of the *points* in the Fig. 4 representation could, in principle, be replaced by horizontal *bars*, of width corresponding to the degree of variation V_A^V/V_B^V found within all compositions of a particular type.

In general, points in the top-left quadrant of Fig. 3(*b*) have $V_A^V/V_B^V < 1$, indicating that a small *A*-ion size favours *A* ions coordinated by *B* ions. Such structures consist, in the main, of *A* ions occupying interstitial sites between densely packed *B* ions. By comparison, points in the opposite (bottom-right) quadrant tend to have V_A^V/V_B^V ratios greater than one. This indicates that a larger relative size of the minority *A* component favours *A*···*A* homoatomic interactions, although the majority of *B* ions do *not* function as interstitial ions here. The dominant trend in Fig. 3(*b*) is an increase in V_A^V/V_B^V from top-left to bottom-right in the diagram.

In Fig. 3(*c*), values of absolute electronegativity difference are used to label the points. In general, a significant ionic character in the bonding arises when $|\chi_A - \chi_B| > 1$, as is observed for salt-like compounds (top, far-left). Otherwise, there is no clear correlation between $|\chi_A - \chi_B|$ values and the positions of points, and electronegativities cannot be used to discriminate between the tendencies of *A* and *B* ions to mix well (bottom-left quadrant) or not (top-right quadrant).

The observed general increase in V_A^V/V_B^V from top-left to bottom-right in Fig. 3(*b*) may be exploited to plot a geometrical–topological structure diagram, as in Fig. 4. Here, the vertical topological axis is a combination of I'_{AA} and I'_{BB}, $I'_{AA} - I'_{BB}$, which increases uniformly from the top-left of Fig. 3(*b*) to bottom-right. Accordingly, in Fig. 4 most of the plotted points are relatively close to the diagonal from bottom left to top right. It may be argued that geometrical (*i.e.* packing) effects are predominant in structural types close to this diagonal. Significant deviations from the diagonal indicate strong interaction-driven (*i.e.* chemical) influences on the structures, as, for example, for compositions *r* (BaS_2), *z* (Ni_2In), *gg* ($NbTe_2$), *hh* ($FeSi_2$), *kk* (As_2Ge) and *pp* (MoS_2, NbS_2).

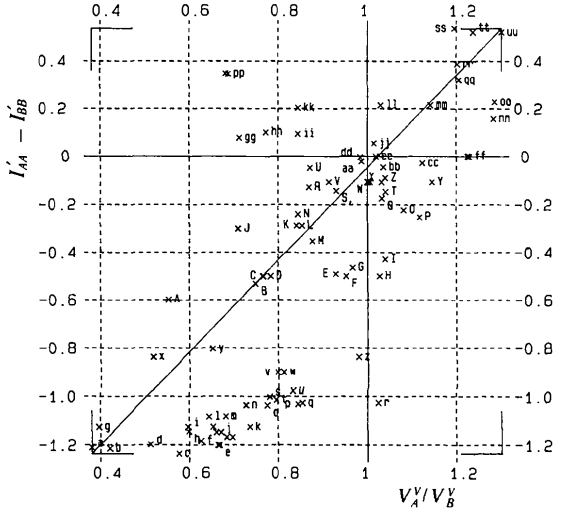

Fig. 4. Geometrical–topological structure diagram for the 85 AB_2 compounds in Table 2. The geometrical axis, V_A^V/V_B^V, is horizontal, with the vertical axis corresponding to the reduced topological variable $I'_{AA} - I'_{BB}$. Many points are observed to be close to the diagonal from bottom-left to top-right of the diagram. Chemical compositions are indicated by characters a–z, A–Z, aa–uu, which can be correlated with the compositions in Table 2.

6. Discussion

Figs. 3 and 4 have been referred to as topological and geometrical–topological structure diagrams, respectively, with indices I'_{AA} and I'_{BB} representing 'topology' and the ratio V_A^V/V_B^V representing 'geometry'. There is scope, however, for refining the method by which the valence fractions of the atoms are distributed over the faces of their respective Voronoi polyhedra, such that the forms of the polyhedra are taken into account in this process. Work is currently in progress to investigate alternative valence-partitioning methods, so that the calculated face-interaction indices reflect the differing interaction strengths of Voronoi faces. Seven purely geometrical methods are under examination: (i) the existing method (even distribution of atomic valences over polyhedral faces); (ii) even distribution of valences over polyhedral vertices; valence distribution over faces in proportion to (iii) facial areas; (iv) facial volume contributions; (v) solid angles subtended by faces at the source atoms of the polyhedra; (vi) an inverse-square variation of source atom-to-face distance, $1/d^2$; (vii) a combination of (v) and (vi). Partitioning of the valences is carried out by the software described in Appendix *B*, based on the quantities calculated in step 9. It would also be instructive to investigate a synthesis of this method and the bond-valence method (Brown & Altermatt, 1985; Brese & O'Keeffe, 1991; O'Keeffe & Brese, 1992). Proceeding from the centre-to-centre distances between neighbouring atoms, total valences for

Table 3. *Comparison of intrinsic face-interaction indices, I'_{AA}, I'_{AB}, I'_{BA} and I'_{BB} between the systems $MgCu_2$, $MgNi_2$ and $MgZn_2$ for different valence-weighting schemes*

	Number based		Area based		Volume based		Solid angle based		$1/d^2$ based	
System/ion	Mg	Cu/Ni/Zn	Mg	Cu/Ni/Zn	Mg	Cu/Ni/Zn	Mg	Cu/Ni/Zn	Mg	Cu/Ni/Zn
$MgCu_2$/Mg	0.75	1.125	0.7443	1.1276	0.7694	1.1153	0.7107	1.1446	0.7021	1.1489
$MgCu_2$/Cu	1.5	0.75	1.2541	0.8729	1.3716	0.8142	1.1446	0.9277	1.2632	0.8684
$MgNi_2$/Mg	0.75	1.125	0.7434	1.1283	0.7682	1.1159	0.7093	1.1454	0.7017	1.1492
$MgNi_2$/Ni	1.5	0.75	1.2535	0.8733	1.3702	0.8149	1.1454	0.9273	1.2654	0.8673
$MgZn_2$/Mg	0.75	1.125	0.7415	1.1292	0.7666	1.1167	0.7072	1.1464	0.7011	1.1465
$MgZn_2$/Zn	1.5	0.75	1.2527	0.8736	1.3683	0.8159	1.1464	0.9268	1.2683	0.8658

each ion could be calculated, leading straightforwardly to valence fractions i_{AA}, i_{AB}, i_{BA} and i_{BB}. This would also be a means of taking chemical information into account retrospectively. Although the Voronoi polyhedra are constructed without regard to differing atomic radii (in order to achieve closure), the bond-valence method could still be used, as it relies solely on centre-to-centre interatomic distances. According to such an approach, the essential rôle of the Voronoi construction would be to establish which atoms to regard as nearest neighbours, just as in the work of Frank & Kasper (1958).*

One of the deficiencies of a structure diagram such as Fig. 3 is that some points would be expected to be closer to one another than they are, whereas others would be expected to be further apart. Relevant examples are the polymorphic systems TiO_2, SiO_2 and FeS_2. The first of these has four polymorphs, anatase, brookite, TiO_2(II) and rutile [points $TiO_2(a)$, $TiO_2(b)$, *o* and *i*, respectively]. However, if indices I'_{AA} and I'_{BB} are to represent 'chemistry', rather than 'topology', it would be desirable, given their identical chemical compositions, for the four points to be closer together, with no other structures intervening. Similar considerations hold for the six polymorphs of SiO_2 analysed: three lie in the cluster of points *p*, *i.e.* high quartz, keatite and low tridymite, with low quartz and low cristobalite represented by points *m* and *l*, respectively. Coesite [labelled SiO_2(coes)] is unique in having a non-zero I'_{AA} index. The two polymorphs of FeS_2, pyrite [$FeS_2(p)$ in Fig. 3(*a*)] and marcasite [$FeS_2(m)$], have adjacent points in the structure diagram.

In other cases, it would be helpful if the method could differentiate more between alternative phases, for example, the three Laves phases, $MgCu_2$, $MgZn_2$ and $MgNi_2$, which have identical number-based face-interaction indices. This would be achieved by taking the geometrical forms of the polyhedra into account in the derivation of these indices, as shown in Table 3. Here, the intrinsic face-interaction indices I' resulting from alternative valence-distribution methods are quoted for each of these systems. Values quoted in Table 2 correspond to the simple number-based method and are also quoted in the left-hand column in Table 3. These have identical values for $MgCu_2$, $MgZn_2$ and $MgNi_2$, *i.e.* $I'_{AA} = 0.75$, $I'_{AB} = 1.125$, $I'_{BA} = 1.5$ and $I'_{BB} = 0.75$. In the column for area-based weighting the valence fractions assigned to polyhedral faces are proportional to facial areas. Volume, solid angle and $1/d^2$-based weightings make use of pyramidal volumes, solid angles and centre-to-face distances, respectively. It is clear from Table 3 that there are variations in calculated indices as the weighting method is changed. However, it is also significant that consistent trends in I' values are observed between the three structures. For example, I'_{AA} values (*i.e.* Mg–Mg interaction indices) vary as follows for all non-simple weighting methods: $I'_{AA}(MgCu_2) > I'_{AA}(MgNi_2) > I'_{AA}(MgZn_2)$. For all indices, values for $MgNi_2$ are intermediate between those of $MgCu_2$ and $MgZn_2$, indicating that the methodology is sensitive to the underlying structural progression from $MgCu_2$ through $MgNi_2$ to $MgZn_2$.

The work described in this paper has laid the foundation for an extensive programme of future work. In the field of inorganic structural chemistry, the method offers new possibilities for investigating relationships between chemical composition and crystal structure. It is significant that structures with different types of bonding (*e.g.* ionic and metallic) can be analysed with the same framework, as well as intermediate cases, such as Zintl phases. Application to molecular systems is also possible, given the generality of the method.

Of fundamental interest is the prospect of deriving quantitative chemical information merely from experimental crystal structural data, without recourse to any prior assumptions or adjustable parameters. The Voronoi analysis provides a more panoramic view of the relationship between chemical composition and crystal structure than that afforded by many current methods, which rely

* The envisaged progression from the simple number-based distribution of valences over polyhedral faces (used here) to a distribution invoking a bond-valence approach mirrors the development of the bond-valence method itself. Essentially, this grew out of Pauling's Second Rule (Pauling, 1960; Thomas, 1991), according to which the numbers of anions coordinating cations determine the 'electrostatic bond strengths' between them. In essence, the bond-valence method permitted the assignment of unequal bond strengths to identical types of ion pairs, by using their separations as indicators of interaction strength. In the Voronoi methodology introduced here, atomic valences are distributed over shared polyhedral faces, rather than cationic valences over shared anions. Thus, the simple number-based distribution is analogous to the topological approach embodied by Pauling's Second Rule.

Table 4. *Representative points of Voronoi edges in the $MgCu_2$ structure*

Special positions		Coordinates of end vertex 1			Coordinates of end vertex 2			Coordinates and special positions a quarter of the way along the edge			Coordinates halfway along the edge		
Edge	End vertices	*x*	*y*	*z*	*x*	*y*	*z*	*x*	*y*	*z*	*x*	*y*	*z*
(96*h*)	(96*g*) (96*g*)	0.1771	0.0208	0.1771	0.0729	0.0729	0.2292	0.1510	0.0339	0.1901 (192*i*)	0.1250	0.0469	0.2031 (96*h*)
(96*g*)	(96*g*) (32*e*)	0.0729	0.0729	0.2292	0.1125	0.1125	0.3875	0.0828	0.0828	0.2688 (96*g*)	0.0927	0.0927	0.3083 (96*g*)
(48*f*)	(96*g*) (96*g*)	0.2292	−0.0729	−0.0729	0.2292	0.0729	0.0729	0.2292	−0.0365	−0.0365 (96*g*)	0.2292	0.0000	0.0000 (48*f*)
(32*e*)	(32*e*) (8*b*)	0.3875	0.3875	0.3875	0.5	0.5	0.5	0.4156	0.4156	0.4156 (32*e*)	0.4438	0.4438	0.4438 (32*e*)

Table 5. *Representative points of Voronoi faces in the $MgCu_2$ structure*

Special position	Atom	Coordinates of atom 1			Coordinates of atom 2			Coordinates and special positions a quarter of the way along the interatomic vector			Coordinates halfway along the interatomic vector		
of face	types	*x*	*y*	*z*	*x*	*y*	*z*	*x*	*y*	*z*	*x*	*y*	*z*
(96*g*)	Mg Cu	0.0000	0.0000	1.0000	0.1250	0.1250	0.6250	0.0312	0.0312	0.9062 (96*g*)	0.0625	0.0625	0.8125 (96*g*)
(48*f*)	Cu Cu	0.6250	0.1250	0.1250	0.6250	−0.1250	−0.1250	0.6250	0.0625	0.0625 (96*g*)	0.6250	0.0000	0.0000 (48*f*)
(16*c*)	Mg Mg	0.0000	0.0000	0.0000	0.2500	0.2500	0.2500	0.0625	0.0625	0.0625 (32*e*)	0.1250	0.1250	0.1250 (16*c*)

heavily on a consideration of interatomic distances and their relationship to idealized atomic radii.

Acknowledgement is made of the use of the EPSRC-funded Chemical Databank Service for part of the work.

APPENDIX *A*
A justification of the procedure for calculating representative points of Voronoi polyhedral elements

In Table 4 the choice of representative points for Voronoi edges in the $MgCu_2$ system is justified, by way of an example. As specified in Table 6, these correspond to special positions (96*h*), (96*g*), (48*f*) and (32*e*) in space group *Fd3m*. The fractional coordinates for one edge of each type are given in Table 4. For illustrative purposes, two alternative representative points for each of the four edge types are considered, one a quarter of the way along the edge (as an arbitrary distance along the edge) and the other half-way along. With respect to the (96*h*) edge, it is seen that the quarter-point occupies a (192*i*) position, so that such a representative point would generate double the required number of equivalent edges in the unit cell. By comparison, the point half-way along the edge occupies a (96*h*) special position and is the appropriate representative point for the edge.

In the case of the (96*g*) edges, which link unlike (96*g*) and (32*e*) vertices, both trial representative points, at a quarter and a half of the distance along the edge, have (96*g*) symmetry. In principle, therefore, any point on such an edge could be taken as a representative point. However, only the adoption of half-way points is adequate for edges linking like vertices, as is also observed for (48*f*) edges.

The choice of representative points of Voronoi faces in $MgCu_2$ is demonstrated in Table 5. As for edges, faces shared by unlike atoms [*i.e.* (96*g*) faces] could be represented by any point along the interatomic vector normal to the face. By comparison, faces shared by like atoms must be represented by points midway along the interatomic vector, as for the (48*f*) and (16*c*) faces.

APPENDIX *B*
Description of the computational procedure applied

Since there is no freely available software for the calculation of Voronoi polyhedra, a new computer program has been developed, based on a schedule given by Mackay (1972). Since the program is to be applied to a variety of chemical systems in the future, many of them more complex than the inorganic systems considered here, it has been designed to run efficiently on a Silicon Graphics 4D/480 Parallel Processor. To this end, explicit parallelization calls have been utilized, these permitting a considerable shortening of execution time. In essence, calculation of the vertex coordinates of the polyhedra is distributed over several (*i.e.* 4–8) processors, with a one-to-one correspondence between polyhedron (or, equivalently, atom in source unit cell) and processor. Once a particular processor has finished calculating a given polyhedron, it moves onto a new one.

The essential steps of the program are as follows.

(*a*) Read in unit-cell parameters and fractional coordinates of all atoms in the unit cell, referred to as the 'source' unit cell.

(*b*) Generate all translationally related atoms within a specified cut-off distance of atoms in the source unit cell, to form the complete set of atoms. Typically $3.5 \leq$ cut-off ≤ 7 Å, depending on the chemical system.

(*c*) Specify an atomic radius for each atom type (see step *e*).

Steps (*d*)–(*i*) are carried out repeatedly in parallel, the sequence being applied to each atom *i* in the source unit cell.

(*d*) Take an atom in the source unit cell and select all possible sets of three coordinating atoms, provided that all four atoms (*i.e.* source atom + coordinating atoms) are not coplanar.

(*e*) For each set of four atoms, calculate the coordinates of the point $[x_V, y_V, z_V]$, which is equidistant from the surface of each atom, at distance D (Fig. 5). This calculation utilizes an algebraic method, in which the following four simultaneous equations are solved

$$(x_V - x_i)^2 + (y_V - y_i)^2 + (z_V - z_i)^2 = (R_i + D)^2, \quad i = 1,4. \qquad (12)$$

Computation of $[x_V, y_V, z_V]$ is simplified by an appropriate axis transformation, whereby x_1, y_1, z_1, y_2 and z_2 become equal to zero. Coordinates $[x_V, y_V, z_V]$ represent a trial Voronoi vertex. If radii R_1–R_4 (as specified in step *c*) are equal, the calculated coordinates correspond to the vertices of an unmodified Voronoi polyhedron, since the distance of the point to each atomic centre is $R + D$. For unequal radii, however, the point $[x_V, y_V, z_V]$ would correspond to the vertex of a modified Voronoi polyhedron similar to a PAV cell, as proposed by Carter (1978), Fig. 1(*c*).* For all calculations of polyhedra in this article, R_1–R_4 have been given equal values, arbitrarily set at 0.2 Å. Note that the magnitude of the uniform radius does not affect the calculated values $[x_V, y_V, z_V]$.

(*f*) Test that this is a valid Voronoi vertex, by ensuring that no atom surface (amongst the complete set of atoms) is closer to $[x_V, y_V, z_V]$ than the distance D.

(*g*) Record which three coordinating atoms (see step 3) have generated $[x_V, y_V, z_V]$ and, in the case of this vertex being a repeat within the same polyhedron, keep a cumulative record of which coordinating atoms have generated it.

(*h*) Once all vertices $[x_V, y_V, z_V]$ have been generated, identify the faces of the Voronoi polyhedron. This procedure is carried out on a logical, rather than a geometrical basis. Since each face of the Voronoi polyhedron being generated is shared with a Voronoi polyhedron of a coordinating atom, the vertices in a given face are those for which the relevant coordinating atom has been involved in their generation. Monitor any deviations in planarity of the polyhedral faces.

(*i*) Calculate the following attributes of the Voronoi polyhedron:

(i) Numbers of corners (vertices), edges and faces, C, E and F, respectively, together with frequencies of faces, f_F, with different numbers of corners, N_C^F.

(ii) Area of each face, A_F (more precisely, area of the projection of the face in its least-squares plane).

(iii) Volume contribution due to each face, V_F. This is calculated by splitting the face into constituent triangles with a common vertex at its centre of coordinates, followed by a summation of the volumes of constituent triangular pyramids with the source atom as the apex (Thomas, 1991).

(iv) Solid angle Φ subtended at the source atom by each face, S_F, employing the constituent triangle methodology in (iii) and the following formula (Mackay, 1972)

$$\Phi = 2\cos^{-1}\{(1 + \cos\alpha + \cos\beta + \cos\gamma)/[4\cos(\alpha/2)\cos(\beta/2)\cos(\gamma/2)]\}. \qquad (13)$$

Here, α, β and γ are the angles subtended at the source atom by the three edges of each constituent triangle.

(v) Distance of each face from the source atom, defined as

$$d_F = (1/2)\{[(X_C - X_S)^2 + (Y_C - Y_S)^2 + (Z_C - Z_S)^2]^{1/2} + R_S - R_C\}. \qquad (14)$$

Here $[x_S, y_S, z_S]$ and $[x_C, y_C, z_C]$ are coordinates of source and coordinating atoms, with R_S and R_C their corresponding radii. For conventional Voronoi polyhedra $R_S = R_C$.

(vi) Total facial area, $A_{F,tot}$ [sum of areas calculated in (ii)].

(vii) Total volume enclosed, $V_{F,tot}$ [sum over all faces of volumes calculated in (iii)].

(viii) Total solid angle subtended at source atom $S_{F,tot}$ [sum over all faces of solid angles calculated in (iv)]. (This calculation is carried out as a check, since the total solid angle must be equal to 4π steradians.)

(ix) Lengths of edges constituting each face, d_E^F, together with angles between adjacent edges, α_E^F.

(x) Centres of coordinates of faces, $[x_F, y_F, z_F]$, *defined* as those points which lie on the lines joining source atoms with neighbouring atoms, midway between the two spherical ion surfaces. In the special case of equal ionic radii, the centres of coordinates of faces correspond to the midpoints of lines joining source and coordinating atoms.

(xi) Centres of coordinates of edges, $[x_E, y_E, z_E]$.

* The situation depicted in Fig. 1(*c*) represents a worse case scenario, since perfect coincidence of PAV faces at vertices is frequently obtained with unequal radii. The software can calculate PAV cells wherever the vertices are coincident, with no provision, as yet, for dealing with indeterminate regions.

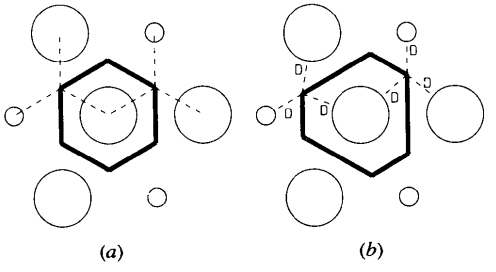

(*a*) (*b*)

Fig. 5. Method used by the software to calculate Voronoi polyhedra: (*a*) for unmodified polyhedra, with vertices equidistant from atom centres; (*b*) for polyhedra similar to PAV cells, with vertices equidistant from atom surfaces.

Table 6. *Geometrical attributes of Voronoi polyhedra of the $MgCu_2$ structure (Ellner & Predel, 1979); space group Fd3m, origin at −43m; $a_o = 7.034$ Å; Mg in (8a) positions, Cu in (16d) positions*

Attribute	Mg polyhedron	Cu polyhedron
$[x_V, y_V, z_V]$	24C in (96*g*) (x, x, z; $x = 0.0729$, $z = 0.2292$) 4C in (32*e*) (x, x, x; $x = 0.3875$) (96*g*): shared by 2 Mg and 2 Cu polyhedra (32*e*): shared by 1 Mg polyhedron and 3 Cu polyhedra (8*b*): shared by 4 Cu polyhedra	12C in (96*g*) 6C in (32*e*) 2C in (8*b*) $[\frac{1}{2}, \frac{1}{2}, \frac{1}{2}]$
$C\|F\|E\|$	28|16|42	20|12|30
$f_F[N_C^F]$	4[6] 12[5]	12[5]
A_F (Å^2)	2.0922 [6] 2.1118 [5]	2.9398 [5] (shared with Cu) 2.1118 [5] (shared with Mg)
V_F (Å^3)	1.0621 [6] 1.0264 [5]	1.2185 [5] (shared with Cu) 1.0264 [5] (shared with Mg)
S_F (4π.steradian)	0.05923 [6] 0.06359 [5]	0.10308 [5] (shared with Cu) 0.06359 [5] (shared with Mg)
d_E (Å)	1.5229 [6] 1.4581 [5]	1.2435 [5] (shared with Cu) 1.4581 [5] (shared with Mg)
$A_{F,tot}$ (Å^2)	33.7099	30.3091
$V_{F,tot}$ (Å^3)	16.5647	13.4691
$S_{F,tot}$ (4π.steradian)	1	1
d_E^F (Å)	6 × 0.897 [6] 1 × 1.451 [5] 2 × 1.181 2 × 0.897	1 × 1.451 [5] (shared with Cu) 2 × 1.371 2 × 1.181 1 × 1.451 [5] (shared with Mg) 2 × 1.181 2 × 0.897
α_E^F (°)	6 × 120 [6] 1 × 112.9 [5] 4 × 106.8	3 × 109.5 [5] (shared with Cu) 2 × 105.8 1 × 112.9 [5] (shared with Mg) 4 × 106.8
$[x_F, y_F, z_F]$	12*F* in (96*g*) (x, x, z; $x = 0.0625$, $z = 0.8125$) (Mg···Cu) 4*F* in (16*c*) $(\frac{1}{8}, \frac{1}{8}, \frac{1}{8})$ (Mg···Mg)	6*F* in (96*g*) (Cu···Mg) 6*F* in (48*g*) ($x, 0, 0$; $x = 0.6250$) (Cu···Cu)
$[x_E, y_E, z_E]$	24*E* in (96*h*) $(\frac{1}{8}, x, \frac{1}{4} - x$; $x = 0.0469$) (2Mg,1Cu) 12*E* in (96*g*) (x, x, z; $x = 0.0927, z = 0.3083$) (1Mg, 2Cu) 6*E* in (48*f*) ($x, 0, 0$; $x = 0.2292$) (1Mg,2Cu)	6*E* in (96*h*) (1Cu,2Mg) 12*E* in (96*g*) (2Cu,1Mg) 6*E* in (48*f*) (2Cu,1Mg) 6*E* in (32*e*) (x, x, x; $x = 0.4438$) (3Cu)
CN(*A*)	15.9997	11.6860
CN(*V*)	15.9964	11.9128
CN(*S*)	15.9854	11.3623
V_A^V/V_B^V	1.2298	

(xii) Effective coordination numbers of the source atom, calculated according to equation (1), with alternative interpretations of s_i: facial areas [CN(*A*)], volume increments of faces [CN(*V*)] or solid angles [CN(*S*)].

Once steps (*d*)–(*i*) have been completed for each source atom, the following calculations are performed serially.

(*j*) Enumeration of total numbers of different elements (*i.e.* corners, edges and faces) of the Voronoi polyhedra in the unit cell, N_C^{uc}, N_E^{uc} and N_F^{uc}, respectively. This is carried out by translating all vertex, edge [step *i*(xi)] and face [step *i*(x)] coordinates, $[x_V, y_V, z_V]$, $[x_E, y_E, z_E]$ and $[x_F, y_F, z_F]$, respectively, to the source unit cell, followed by elimination of repeats (*i.e.* superimposed polyhedral elements).

(*k*) Calculation of Voronoi polyhedral volume ratios, *e.g.* V_A^V/V_B^V in a binary compound A_mB_n and the sum of the polyhedral volumes of all source atoms, which must be equal to the unit cell volume.

(*l*) Calculation of face-based interaction indices.

APPENDIX *C*
Application of the computational procedure to the $MgCu_2$ system

*C*1. *Geometrical attributes*

Geometrical attributes of the $MgCu_2$ structure, which has been chosen as an example, are given in Table 6. The notation in the table has been defined in Appendix

B, with the meanings of $[x_F, y_F, z_F]$ and $[x_E, y_E, z_E]$ elucidated in the main text and in Appendix A.

C2. Topological attributes: example calculations of i, I and N^i values

The structures of NaCl and $MgCu_2$ may be considered, in order to illustrate the calculation of face-interaction indices. The structure of NaCl belongs to space group 225 ($Fm3m$), with Na^+ ions on (4a) and Cl^- ions on (4b) sites. Thus, $Z = 4$, $m = 1$ and $n = 1$. By comparison, the $MgCu_2$ structure belongs to space group 227 ($Fd3m$), with Mg ions in (8a) and Cu ions in (16d) positions (Ellner & Predel, 1979). Thus, $Z = 8$, $m = 1$ and $n = 2$. In NaCl, the Voronoi polyhedra of both Na^+ and Cl^- ions are cubes, *i.e.* 8|6|12 6[4], with vertices occupying (8c) positions in space group 225. In $MgCu_2$ the Mg polyhedra are of the form 28|16|42 4[6] 12[5] (hexakaidecahedra), with the Cu polyhedra of dodecahedral form, 20|12|30 12[5] (Table 6).

In NaCl, all Voronoi cube faces are shared with cubes of the other atom type, *i.e.* $i_{AA} = 0$, $i_{AB} = 1$, $i_{BA} = 1$ and $i_{BB} = 0$. Thus, according to (2) and (3), $I_{AA} = 0$, $I_{AB} = 4$, $I_{BA} = 4$ and $I_{BB} = 0$. In $MgCu_2$, the hexagonal faces of the Mg polyhedra are shared with other Mg polyhedra, whereas all pentagonal faces are shared with Cu polyhedra. Consequently, $i_{AA} = 4/16 = 0.25$ and $i_{AB} = 0.75$. Six of the faces of the Cu polyhedra are shared with other Cu polyhedra, the other six being shared with Mg polyhedra. Thus, $i_{BA} = i_{BB} = 0.5$, with face-interaction indices I_{AA}, I_{AB}, I_{BA} and I_{BB} equal to 2, 6, 8 and 8, respectively.

Numbers of interactions of different types may be directly inferred from (5), (6) and (7). Thus, in NaCl: $N^i_{AA} = I_{AA}F_A/2 = 0$, $N^i_{AB} = I_{AB}F_A = I_{BA}F_B = 24$, $N^i_{BB} = I_{BB}F_B/2 = 0$; in the $MgCu_2$ structure: $N^i_{AA} = I_{AA}F_A/2 = 2 \times 16/2 = 16$, $N^i_{AB} = I_{AB}F_A = 6 \times 16 = I_{BA}F_B = 8 \times 12 = 96$, $N^i_{BB} = I_{BB}F_B/2 = 8 \times 12/2 = 48$. These numbers are in agreement with the $[x_F, y_F, z_F]$ data in Table 6.

References

Brese, N. E. & O'Keeffe, M. (1991). *Acta Cryst.* B**47**, 192–197.
Brown, I. D. & Altermatt, D. (1985). *Acta Cryst.* B**41**, 244–247.
Carter, F. L. (1978). *Acta Cryst.* B**34**, 2962–2966.
Dirichlet, G. L. (1850). *Crelle's J.* **40**, 209–227.
Ellner, M. & Predel, B. (1979). *J. Solid State Chem.* **30**, 209–217.
Fischer, W. & Koch, E. (1979). *Z. Kristallogr.* **150**, 245–260.
Fischer, W., Koch, E. & Hellner, E. (1971). *Neues Jahrb. Mineral. Monatsh.* pp. 227–237.
Frank, F. C. & Kasper, J. S. (1958). *Acta Cryst.* **11**, 184–190.
Haüy. R.-J. (1822). Traité de Crystallographie, Paris.
Hoppe, R. (1970). *Angew. Chem.* **82**, 7–16.
Kepler, J. (1611). *Strena seu de nive sexangula.* Francofurti ad Moenum.
Koch, E. & Fischer, W. (1980). *Z. Kristallogr.* **153**, 255–263.
Mackay, A. L. (1972). *J. Microsc.* **95**, 217–227.
Nesper, R. (1991). *Angew. Chem. Int. Ed. Engl.* **30**, 789–817.
Niggli, P. (1927). *Z. Kristallogr.* **65**, 391–415.
Niggli, P. (1928). *Z. Kristallogr.* **68**, 404–466.
O'Keeffe, M. & Brese, N. E. (1992). *Acta Cryst.* B**48**, 152–154.
Pauling, L. (1960). *The Nature of the Chemical Bond*, 2nd ed. Ithaca: Cornell University Press.
Pettifor, D. G. (1986). *J. Phys. C*, **19**, 285–313.
Senechal, M. (1990). *Crystalline Symmetries: An Informal Mathematical Introduction.* Bristol: Adam Hilger.
Thomas, N. W. (1991). *Acta Cryst.* B**47**, 180–191.
Voronoi, G. (1908). *Crelle's J.* **133**, 97–178.